Theoretical and Applied Climatology (2020) 142:1283–1293
https://doi.org/10.1007/s00704-020-03366-2

ORIGINAL PAPER

Potential dynamic of irrigation water requirement for rice across Northeast China

Lei Zhang[1] · Fangying Tan[1] · Sen Li[1] · Zhiguo Huo[2,3]

Received: 1 March 2020 / Accepted: 25 August 2020 / Published online: 14 September 2020

Abstract

Sufficient water is essential for maintaining rice production yields, but precipitation and ground water generally do not meet the requirements for rice growth. Irrigation is therefore necessary and the quantity of irrigation water requirement (IWR) is also highly dependent on climatic alterations. We utilized an ensemble of 20 fine-resolution downscaled global climate models to characterize the future dynamics of IWR across Northeast China, under two representative concentration pathway scenarios (RCP4.5 and RCP8.5). Crop evapotranspiration was a critical factor in IWR determinations and was estimated through the Hargreaves model. The model was recalibrated to optimize its performance and this resulted in normalized root mean squared errors of < 10%. Based on reliable crop evapotranspiration and effective precipitation data in baseline (1976–2005) and future periods (2036–2065 and 2070–2099), IWR decreased from southwestern Heilongjiang and western Jilin to the southeastern and northeastern areas. The IWR displayed a general increasing trend but overall the tendency decreased from west to east. The western areas were exposed to higher magnitudes of IWR increases, indicating that the water deficit for rice would be more severe in these regions. IWR levels increased with time slice under RCP8.5 relative to RCP4.5. The predicted IWR changes in future periods were greatest for Heilongjiang, followed by Jilin and Liaoning. In addition, Heilongjiang was predicted to have the most stable IWR in the future. These predictions of IWR dynamics highlight sensitive areas prone to water deficits and can serve as guides for specific irrigation schedules in the different rice growing regions across Northeast China.

1 Introduction

Water is an essential resource that has a broad impact on socioeconomic systems and natural ecosystems (Schaldach et al. 2012). Water usage by cultivated crops is a primary issue facing modern agriculture and changing patterns of precipitation make regional and local water scarcity events more probable around the world (Gosling and Arnell 2016; Mancosu et al. 2016; Wang et al. 2017). Driven by climate change, there are serious risks of water shortage in China, even in the places with relatively abundant water resources including precipitation, such as the southern China mainland (Wang et al. 2014; Ye et al. 2015; Yu et al. 2016; Gao et al. 2018). In general, water is far from sufficient for crop growth and irrigation is thus necessary to maintain production. Currently, agricultural irrigation water accounts for > 70% of total domestic water consumption in China (Han et al. 2019). In particular, rice is one of the most water-consuming crops and China produces 32% of the total worldwide production during 1981–2018 (FAO 2020). Therefore, careful regulation of irrigation water resources is essential to ensure sustainable rice production.

There are two factors to the efficient use of irrigation water to optimize water resources. One is to optimize irrigation systems and in practice, a number of approaches have been used including traditional, shallow wet, intermittent, furrow, drip, and controlled irrigation. The optimal procedure for rice water-use efficiency depends on local and regional soil composition and precipitation patterns (He et al. 2013; Zhang et al. 2013; Wang et al. 2016). The second factor is determination on the actual amount of irrigation water needed for rice cultivation, the irrigation water requirement (IWR). IWR is a tool

Electronic supplementary material The online version of this article (https://doi.org/10.1007/s00704-020-03366-2) contains supplementary material, which is available to authorized users.

✉ Zhiguo Huo
huozg@cma.gov.cn

[1] National Meteorological Center, Beijing 100081, China

[2] Chinese Academy of Meteorological Sciences, Beijing 100081, China

[3] Collaborative Innovation Center on Forecast and Evaluation of Meteorological Disasters, Nanjing University of Information Science & Technology, Nanjing 210044, China

that in general encompasses the water requirements for rice and has been increasingly used as a predictive tool (Wang et al. 2014, 2017; Ding et al. 2017; Han et al. 2019). Deterministic tools and methods have been developed to assist in irrigation planning and water management. Crop growth simulation models, merging dynamic and mechanistic properties of crop growth, are widely used proposed to calculate the IWR over a growing period. For example, ORYZA2000 and ORYZA v3 are two common simulation models for IWR calculations across rice cultivation regions in China (Wang et al. 2017; Ding et al. 2017, 2020). The soil water balance method is another traditional method for calculation IWR and has also been applied to rice cultivation (Shahid 2011; Mancosu et al. 2016).

The IWR is highly dependent on associated climatic conditions and this becomes more important as global climatic patterns affect regional and local water availability (Wang et al. 2014; Nie et al. 2019). This will be inevitably ongoing in the future. Global climate model (GCM) and regional climate model (RCM) are the current most useful tools to estimate future dynamic IWR predictions for rice (Gosling and Arnell 2016; Ding et al. 2017). In the outputs derived from these models, temperature and precipitation have been closely linked to the actual observational data (Donat et al. 2017; Sangelanton et al. 2019). There are still small biases in these outputs but they are superior to other simulations, e.g., net radiation and wind speed (Liu and Sun 2016). These differences in the integrity and accuracy of the data limit the use of one particular method such as a crop growth simulation model that requires multivariable inputs and may generate greater uncertainty than the method using reliable inputs. Overall, the input of fewer variables is most appropriate for quantifying IWR.

A simpler soil water balance method that couples crop evapotranspiration and effective precipitation has been proposed to quantify IWR (Ye et al. 2015). Crop evapotranspiration has been evaluated by a variety of methods, such as Penman-Monteith, Thornthwaite, Holdridge, Hargreaves, Priestley, and Taylor (Bormann 2011; Feng et al. 2017; Zhang et al. 2020b). The Penman-Monteith model requires the most detailed data inputs and this has precluded in satisfactory estimation of future evapotranspiration. It is thus reasonable and necessary to choose proper models before they are applied to a specific region.

Until now, efforts to include the impacts of climate change on IWR calculations have been used across the southern rice-plantation areas of China but not for Northeast China (NEC). NEC encompasses the largest plain areas and is a significant base of rice production for China. The planted areas and yields of single-season rice in NEC have increased over the past decades, and on average account for 21.4 and 20.9% in total single-season rice planted areas and yields in China during 2001–2017, in accordance with the statistics from the National Bureau of Statistics of China. The inclusion of IWR dynamics into irrigation scheduling is important to maintain current production yields. This can be accomplished under two representative concentration pathway scenarios, moderate greenhouse gas emissions (RCP4.5) and highest greenhouse gas emissions (RCP8.5), along with utilization of 20 fine-resolution downscaled GCMs as the primary tools to predict potential IWR changes. The current study describes a method to calculate IWR dynamic processes into future models of rice production and is especially important considering the current state of climatic alterations now being experienced across the globe.

2 Material and methods

2.1 Study region and datasets

Our study area encompassed the northeastern China mainland, including Heilongjiang (HLJ), Jilin (JL), and Liaoning (LN) provinces (Fig. 1). This region involved warm, mid, and cold temperate zones from south to north, respectively, resulting in hot and rainy summers, and cold and dry winters. Annual temperatures during 1981–2010 ranged from − 3.8 to 11.3 °C, precipitation between 370 and 1078 mm, and hours of sunshine varied between 2136 and 2910 h. The rice growing season extended from May to September during most years.

We utilized 20 GCMs that were involved in phase five of the Coupled Model Intercomparison Project (CMIP5), i.e., ACCESS1-0, BNU-ESM, CCSM4, CanESM2, CNRM-CM5, CSIRO-Mk3-6-0, GFDL-CM3, GFDL-ESM2G, GFDL-ESM2M, inmcm4, HadGEM2-ES, IPSL-CM5A-LR, IPSL-CM5A-MR, MIROC5, MIROC-ESM, MIROC-ESM-CHEM, MPI-ESM-LR, MPI-ESM-MR, MRI-CGCM3, and NorESM1-M (Zhang et al. 2020a). The datasets included daily mean near surface air temperature (T_{mean}), maximum near surface air temperature (T_{max}), minimum near surface air temperature (T_{min}), and precipitation (P) during the recorded period (1961–2005) and for future periods (2006–2100) under RCP4.5 and RCP8.5 scenarios. Limited by the coarse resolution for the raw GCMs, a downscaling technique was necessary to generate fine-resolution simulations. The statistical downscaling method we used was the bias correction spatial disaggregation, which was applied to daily outputs (Thrasher et al. 2012; Werner and Cannon 2015). Therefore, T_{mean}, T_{max}, T_{min}, and P were reproduced across the study region for 1961–2005 and 2006–2100 under RCP4.5/8.5 for the 20 GCMs at a 0.25° × 0.25° resolution.

Daily observations including T_{mean}, T_{max}, T_{min}, P, wind speed, sunshine duration, and actual vapor pressure were recorded during 1961–2005 at 184 meteorological stations (Fig. 1). These records had been strictly controlled by the China Meteorological Data Sharing Service System to maintain internal long-term consistency and homogeneity.

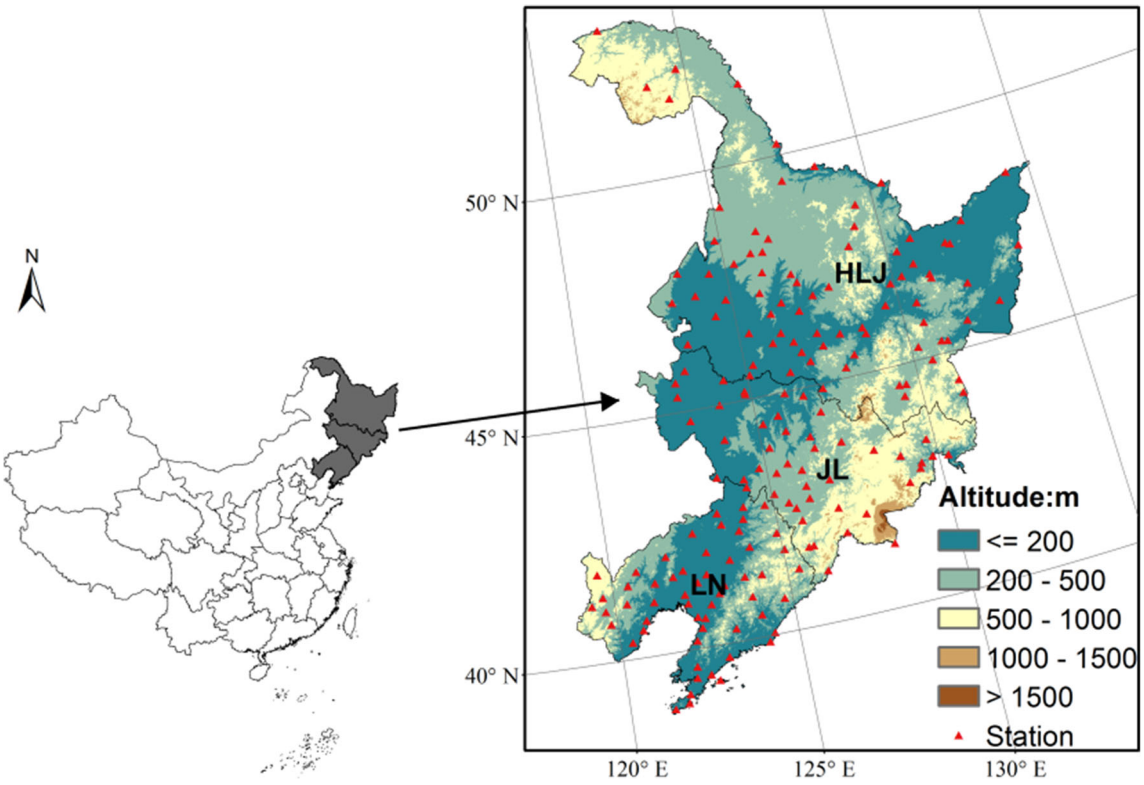

Fig. 1 The location of study area

2.2 The calculation of irrigation water requirement

IWR for rice was defined as the deficit of effective precipitation (EP) relative to crop water requirement (CWR) expressed as:

$$\mathrm{IWR} = \sum_{i=1}^{n} \mathrm{CWR}_i - \sum_{i=1}^{n} \mathrm{EP}_i \tag{1}$$

where CWR_i and EP_i are the daily CWR and EP at day i during the calculated period. Daily CWR was quantified as follows:

$$\mathrm{CWR} = k_c \times \mathrm{ET}_0 \tag{2}$$

where k_c is the crop coefficient and ET_0 is the potential evaporation. The value for k_c was obtained from prior knowledge (Huang et al. 2015) and assigned 1.05, 1.12, 1.20, 1.20, and 0.75 to May (May), June (Jun), July (Jul), August (Aug), and September (Sep), respectively. To generate reliable outputs from statistical downscaled GCMs, the ET_0 was estimated using the Hargreaves model (Hargreaves and Allen 2003) which was a simple and practical method based on daily temperatures as follows:

$$\mathrm{ET}_{0\text{–Har}} = \frac{k}{\lambda}(T\,\mathrm{max} - T\mathrm{min})^{0.5}(T\mathrm{mean} + 17.8)R_a \tag{3}$$

where λ is latent heat of vaporization (2.45 $\mathrm{MJ{\cdot}kg^{-1}}$) and k is the adjusted coefficient taking 0.0023 as the initial value. Ra is extraterrestrial radiation quantified as:

$$R_a = \frac{24 \times 60}{\pi} G_{sc} d_r [\omega_s \sin(\varphi)\sin(\delta) + \cos(\varphi)\cos(\delta)\sin(\omega_s)] \tag{4}$$

where G_{sc} is solar constant (0.082 $\mathrm{MJ{\cdot}m^{-2}{\cdot}min^{-1}}$); d_r is the average distance between sun and earth; ω_s is the angle of sunrise (rad); φ is latitude (rad); and δ is magnetic declination of sun (rad). d_r, ω_s, and δ are expressed as:

$$d_r = 1 + 0.033\cos\left(\frac{2\pi J}{365}\right) \tag{5}$$

$$\delta = 0.409\left(\frac{2\pi J}{365} - 1.39\right) \tag{6}$$

$$\omega_s = \arccos[-\tan(\varphi)\tan(\delta)] \tag{7}$$

where J is the Julian day, ranging from 1 (Jan 1) to 365 or 366 (Dec 31).

It was previously determined that the value of k in the Hargreaves model varied by locality implying that it was necessary to first calibrate k (Hargreaves and Allen 2003; Feng et al. 2017). To address this, ET_0 derived from the Penman-Monteith model was accepted as the reference (Donohue et al. 2010; Zhao and Dai 2017).

$$\mathrm{PET_{PM}} = \frac{0.408\Delta(R_n - G) + \lambda \frac{900}{T\mathrm{mean} + 273} U_2(e_s - e_a)}{\Delta + \gamma(1 + 0.34u_2)} \quad (8)$$

where R_n is net radiation (MJ·m^{-2}·day^{-1}); G is soil heat flux density (MJ·m^{-2}·day^{-1}); e_s is saturation vapor pressure (kPa); e_a is actual vapor pressure (kPa); Δ is slope of the saturation vapor pressure function (kPa·°C^{-1}); γ is psychometric constant (kPa·°C^{-1}); and u_2 is wind speed at 2 m height (m·s^{-1}). In the routine observation from meteorological station, wind speed was measured at 10 m height. u_2 was thus calculated by the following equation:

$$U_2 = U_{10} \frac{4.87}{1n(67.8z - 5.42)} \quad (9)$$

where u_{10} is the measured wind speed at 10 m height (m·s^{-1}) and z is the measured height, which is 10 m here.

Given that ET_0 from the Penman-Monteith model was available, the value of k in the Hargreaves model was calibrated as follows: (1) ET_0 from Penman-Monteith during May–Sep in 1976–2005 was obtained from observations and separately calculated for each station; (2) ET_0 from Penman-Monteith was interpolated to gridded values at a resolution of 0.25° × 0.25° same to downscaled GCMs; (3) gridded ET_0 from Hargreaves estimated from an ensemble of 20 GCMs was compared with gridded ET_0 from Penman-Monteith to adjust the coefficient k. Based on this adjusted k value, the ET_0 from Hargreaves during May–Sep was recalculated during 1976–2005. The normalized root mean squared error (NRMSE) was recognized as the metric to validate the performance of ET_0 from Hargreaves when comparing with the ET_0 from Penman-Monteith.

As another important factor determining IWR, EP is the fraction of the total precipitation available for rice. It was quantified as previously described (Döll and Siebert 2002) as:

$$\mathrm{EP} = \begin{cases} \frac{P \times (4.17 - 0.2P)}{4.17}, & P < 8.3 \\ 4.17 + 0.1 \times P, & P \geq 8.3 \end{cases} \quad (10)$$

where P is daily total precipitation (mm·day^{-1}). The daily EP values were summed during a single period.

2.3 Spatial and temporal analysis method

It had been proved that the reproduced simulations from statistical downscaling GCMs were consistent and agreed with observations from previous studies (Zhang et al. 2020a). The products of 20 downscaled models were merged to an ensemble dataset using the multi-model arithmetic mean ensemble method, and performed better than individual model and reduced uncertainties (Li et al. 2015; Wang et al. 2017). Here, three variables (i.e., tmean, tmax-tmin, EP) used to calculate IWR were evaluated across the northeastern China mainland, as represented in Fig. S1. Comparisons of regional tman, tmax-tmin, and EP in 1976–2005 estimated from downscaled models ensemble and observation elucidated that the variability between them was consistent and the difference was in a small bias, implying the ensemble outputs were reliable to be used in this study. Moreover, it was clear that tmean and EP were generally detected in an increasing trend, but tmax-tmin was in a non-significant trend. The trend of the three variables could contribute to explain the potential changes of IWP in the spatial and temporal patterns under RCP4.5 and RCP8.5 scenarios. The historical period of 1976–2005 (P0) from GCMs was taken as baseline, and future periods were divided into two periods, namely the mid-term period of 2036–3065 (P1) and late-term period of 2070–2099 (P2). To quantify the IWR trends, the Thiel-Sen method (Sen 1968; Thiel 1950) was adopted at grid and provincial scales. In addition, the coefficient of variation (CV) was used to express IWR stability that was defined as the degree of deviation from a standard value over a certain period.

3 Results

3.1 Calibration and validation of the Hargreaves model

The Hargreaves model was calibrated by the calibration of k using ET_0 from Hargreaves compared with ET_0 from Penman-Monteith. The calibrated k values were spatially distinct and decreased from west to east over the study area with a magnitude of 0.0021–0.0024 in southwestern HLJ and western JL. ET_0 was then reobtained from the Hargreaves model with the use of calibrated k and validated by comparing it with ET_0 from Penman-Monteith. The NRMSE values for the two ET_0 values were < 10% in the majority of the study area with only 10–14% in scattered locals indicating that Hargreaves was an acceptable method to estimate ET_0 (Fig. 2).

3.2 Potential spatial-temporal IWR alterations

The availability of reliable P and ET_0 data allowed reliable estimation of IWR for rice. During May–Sep there were obvious spatial differences. In baseline, the highest IWR (> 500.00 mm) was located in southwestern HLJ and western JL. From these areas, IWR decreased with the lowest magnitude (< 100.00 mm) in southeastern LJ and eastern LN. IWR in HLJ varied in a decreasing-to-increasing from west to east. There was a similar spatial pattern of IWR in future periods with only small differences between them and baseline. Overall, IWR decreased in 2036–2065 under RCP4.5 but increased in other periods, with larger magnitude under RCP8.5 than RCP4.5 (Fig. 3).

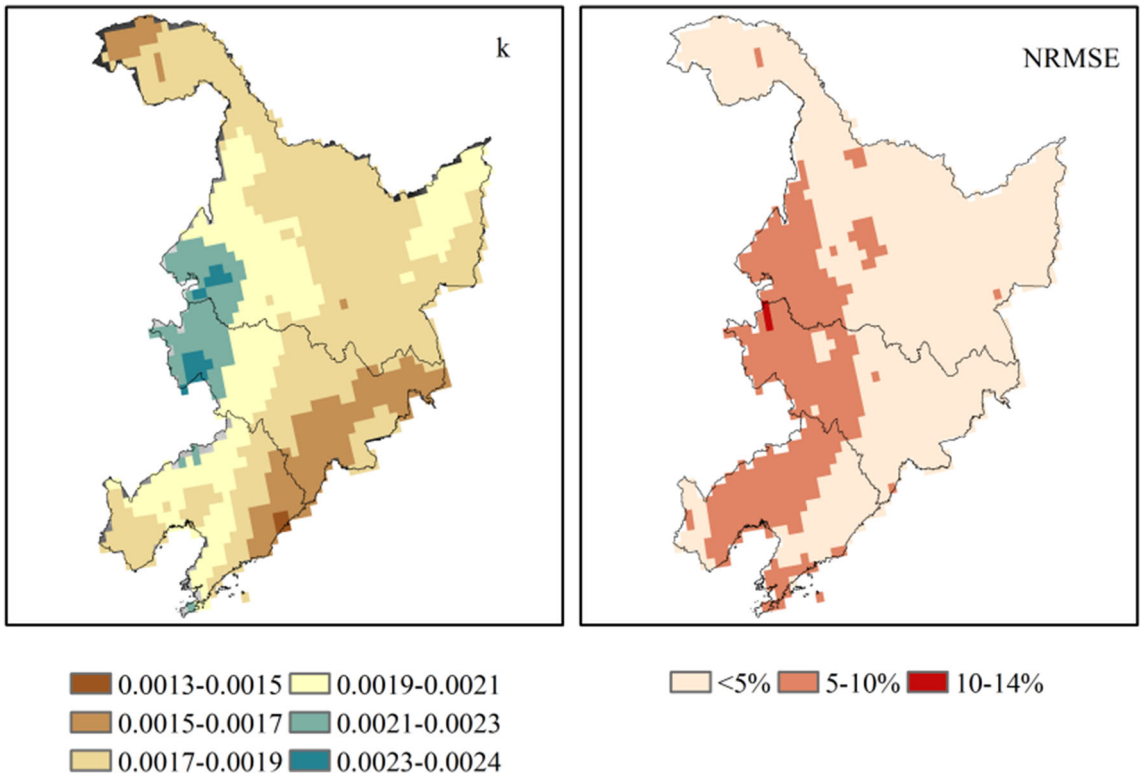

Fig. 2 Calibrated *k* and NRMSE for the Hargreaves model

Potential alterations for IWR were also examined for growth time slices (Fig. S2–S6). It was similar that IWR decreased from western areas (southwestern HLJ and western JL) to southeastern and northeastern areas in different months from May to Sep. This spatial pattern was consistent for both baseline and future periods, and the changes between them were small. A relative positive change of IWR occurred in the latter periods and a larger value was found for RCP8.5 relative to RCP4.5. IWR in Sep was generally < 50.00 mm, much smaller than all other months in which IWR was consistently < 30.00 mm in the southeastern areas (eastern LJ and eastern LN). In western areas (southwestern HLJ and western JL), IWR was > 100.00 mm. Overall, comparisons of IWR grouped by month indicated that IWR was ranked as Jun > May > Jul > Aug > Sep.

The baseline IWR indicated increases during May–Sep from the southwestern areas to northeastern areas, and the tendency ranged from < − 0.8 to 0.4–0.8 mm·a^{-1}. Although the spatial patterns differed for the monthly IWR values, in general they increased from south to north (Fig. 4). In the future periods, IWR generally tended to increase during May–Sep in the respective ranges of 0.20–0.80 and 0.40–1.00 mm·a^{-1} under RCP4.5 and RCP8.5. Additionally, a trend of 0–0.60 mm·a^{-1} in monthly IWR was expected and greater for RCP8.5 than RCP4.5.

3.3 Regional change of IWR

When gridded IWR was integrated to the province value, provincial IWR dynamic was explored. In LN, IWR in baseline was 317.34, 85.74, 82.73, 61.65, 60.89, and 26.32 mm, for May–Sep, May, Jun, Jul, Aug, and Sep, respectively. Relative to baseline, IWR during May–Sep in 2036–2065 and 2070–2099 was changed by − 4.63 and 1.46% under RCP4.5, and − 0.30 and 3.09% under RCP8.5, respectively (Table 1). A general negative change of IWR in the future periods was detected in Jul, Aug, and Sep, while a positive change was recorded in May and June. Regarding JL, IWR was 288.27, 77.62, 74.00, 61.50, 55.92, and 19.23 mm in baseline, for May–Sep, May, Jun, Jul, Aug, and Sep, respectively. A positive change of IWC during May–Sep was identified for 2070–2099 under RCP4.5, as well as 2036–2065 and 2070–2099 under RCP8.5. IWR for each month was generally positive in 2070–2099 under RCP4.5 and RCP8.5. For HLJ, IWR in baseline was 298.27, 76.04, 82.97, 75.06, 54.39, and 9.81 mm, for May–Sep, May, Jun, Jul, Aug, and Sep, respectively. Similar to JL, IWR for HLJ during May–Sep and individual month was generally positive in 2070–2099 under RCP4.5, as well as 2036–2065 and 2070–2099 under RCP8.5. Overall, change of IWR in 2070–2099 relative to 1976–2005 was larger than that in 2035–2065 relative to 1976–2005.

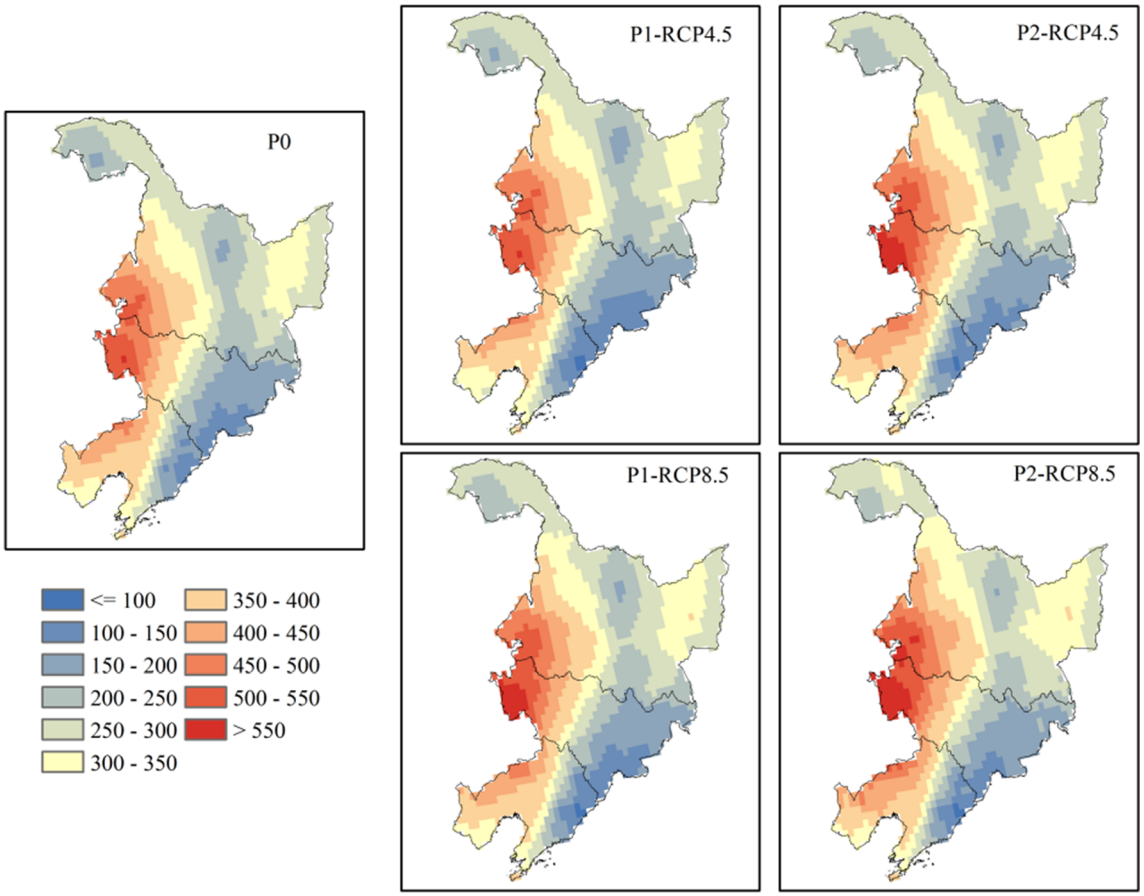

Fig. 3 Potential change of IWR in different periods during May–Sep (P0, P1, and P2 represent 1976–2005, 2036–2065, and 2070–2099, respectively; unit is mm)

Comparisons of IWR by province indicated a positive trend for May–Sep, May, and Jun (Fig. 5). In addition, this tendency was greater under RCP8.5 relative to RCP4.5. IWR was characterized by fluctuation within periods and CV for May–Sep under RCP8.5 was generally larger than for RCP4.5 (Fig. 6). The CV in May, Jun, and Jul was smaller than that in Aug and Sep. A smaller CV in Jun, Jul, Aug, and May–Sep was demonstrated in HLJ, relative to LN and JL. Overall, the IWR changes were largest in HLJ, followed by JL and LN. Moreover, the change of IWR was larger under RCP8.5 and this value in May–Sep in 2070–2099 was more than 2 times greater than that calculated under RCP4.5.

4 Discussion

Increases in temperatures and altered patterns of precipitation inevitably affected future water and irrigation requirements for rice. Climate simulations for these elements were therefore necessary for projecting the dynamic of water and irrigation requirement for rice. The ET_0 taken from the Hargreaves model was a good reproduction of temperatures derived from downscaling GCM. However, it was necessary to calibrate the Hargreaves model according to locality (Hargreaves and Allen 2003). Following calibration, ET_0 from Hargreaves was consistent with reference values and with previous publications (Feng et al. 2017; Zhang et al. 2020b). This confirmed that the calibrated Hargreaves model outperformed raw model results. Crop models have been used to estimate yields and biomass as well as ET (Wang et al. 2014, 2017) and have taken the bias between simulation and observation or reference into account as inevitable. For example, comparisons between simulated and measured ET indicated a substantial 6 to 20% discrepancy (Boudhina et al. 2019). Therefore, our Hargreaves model containing < 10% NRMSE was acceptable and could be used to obtain reliable ET_0, and CWR values for rice.

Based on reliable EP and CWR values, IWR could be dynamically explored for baseline and future periods. It was found similar spatial patterns of IWR during rice growing periods that decreased from western areas (southwestern HLJ and western JL) to southeastern and northeastern areas, which was consistent with previous studies that identified IWR decreased in these same areas (Huang et al. 2015). In addition, there was a special pattern of decrease-to-increase from west to center to east in HLJ that was also consistent with a previous study (Nie et al. 2019). Over time, a general

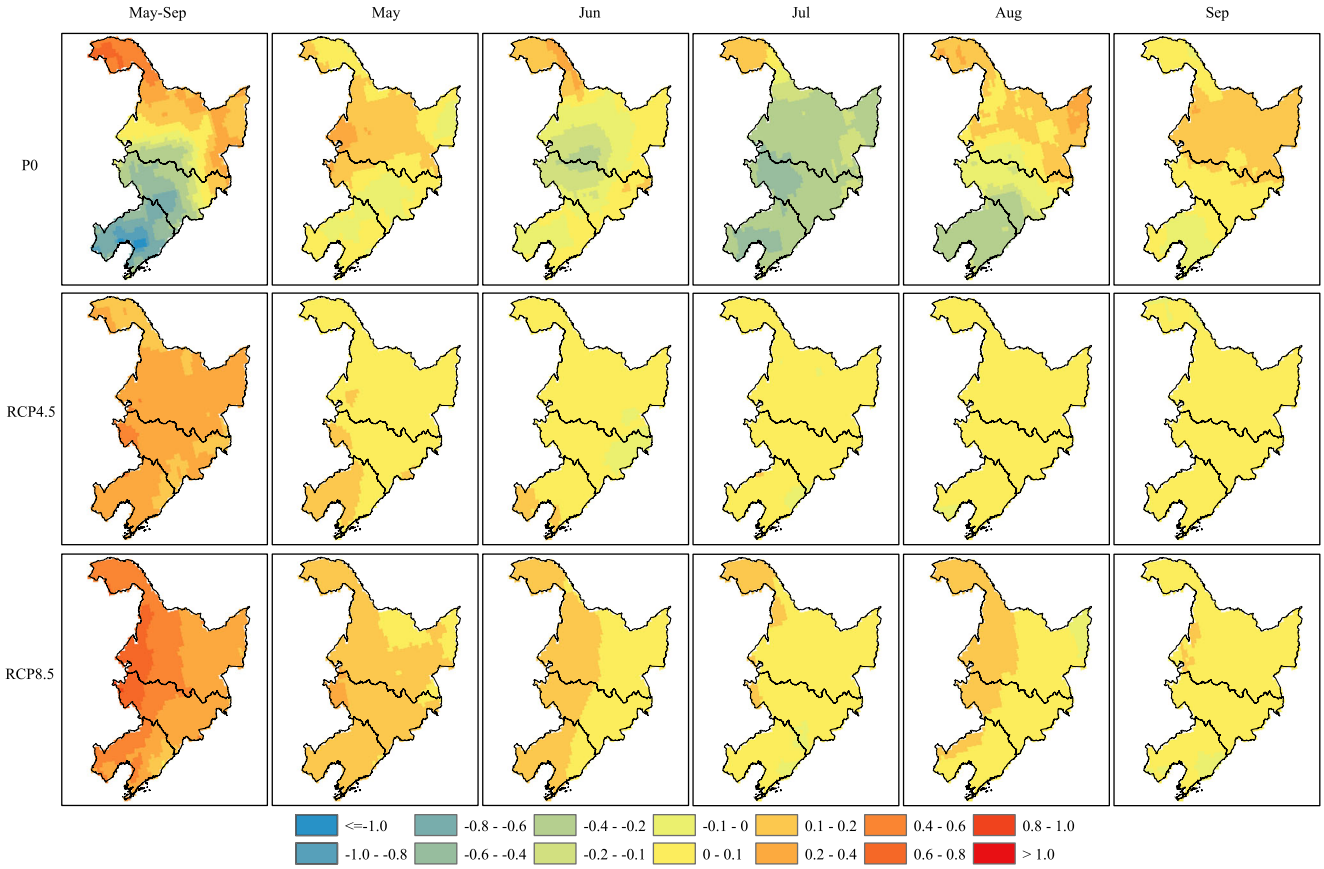

Fig. 4 Tendency of IWR in different periods (P0 represents 1976–2005; unit is mm·a^{-1})

Table 1 IWR in baseline and percent change in future periods relative to baseline in provinces

Province	Period	P0 (mm)	RCP4.5 (%)		RCP8.5 (%)	
			P1 (%)	P2	P1	P2
LN	May	85.74	0.49	6.35	0.13	8.29
	Jun	82.73	−4.99	3.95	5.34	8.72
	Jul	61.65	−10.99	−5.35	−3.31	−2.06
	Aug	60.89	−6.01	−2.31	−5.47	−3.36
	Sep	26.32	−2.06	2.43	−0.37	−4.52
	May–Sep	317.34	−4.63	1.46	−0.30	3.09
JL	May	77.62	2.00	6.76	0.60	8.42
	Jun	74.00	−4.41	3.17	6.71	9.73
	Jul	61.50	−8.31	−3.65	−1.54	2.25
	Aug	55.92	−1.68	3.96	−0.59	3.22
	Sep	19.23	0.56	6.19	9.14	12.08
	May–Sep	288.27	−2.66	3.04	2.05	6.67
HLJ	May	76.04	2.04	5.19	2.39	9.12
	Jun	82.97	0.15	3.23	5.95	9.90
	Jul	75.06	−5.68	−2.41	−0.38	2.75
	Aug	54.39	−0.13	5.47	3.30	5.19
	Sep	9.81	−4.79	8.11	11.24	36.03
	May–Sep	298.27	−1.05	2.88	3.14	7.90

increasing trend for IWR was detected across the study region that displayed different magnitudes and more significant under RCP8.5 relative to RCP4.5. The predictions indicated IWR increased across NEC at rates of 0.01–0.10 mm·day^{-1} in 2046–2065 with greater levels under high over low emission (Zhu et al. 2015). This reinforced our data for IWR spatial-temporal changes although the particular details could vary between studies. For example, western areas had been exposed to higher magnitudes and increased IWR trends indicating that the water deficit for rice would be more severe. However, previous investigations reported a 5-m decline of the shallow groundwater level and a large area of cone of depression in the central and western regions of JL (Fan et al. 2009). The ongoing demand for IWR and declining water resources implied that effective irrigation schedules should be developed for maintaining rice production.

The potential alterations in IWR were the result of the use of CWR and EP data (Nie et al. 2019). To explain these changes, we separately extracted contributions from EP and CWR (Tables 2 and 3). It was clear that positive CWR and EP values were predicted for the future relative to baseline. Recent studies had also suggested that increased temperatures and altered rainfall patterns were likely to cause a significant increase in IWR (Ye et al. 2015). Following climate change, rising temperatures might be the primary reason for the increase in CWR. This had

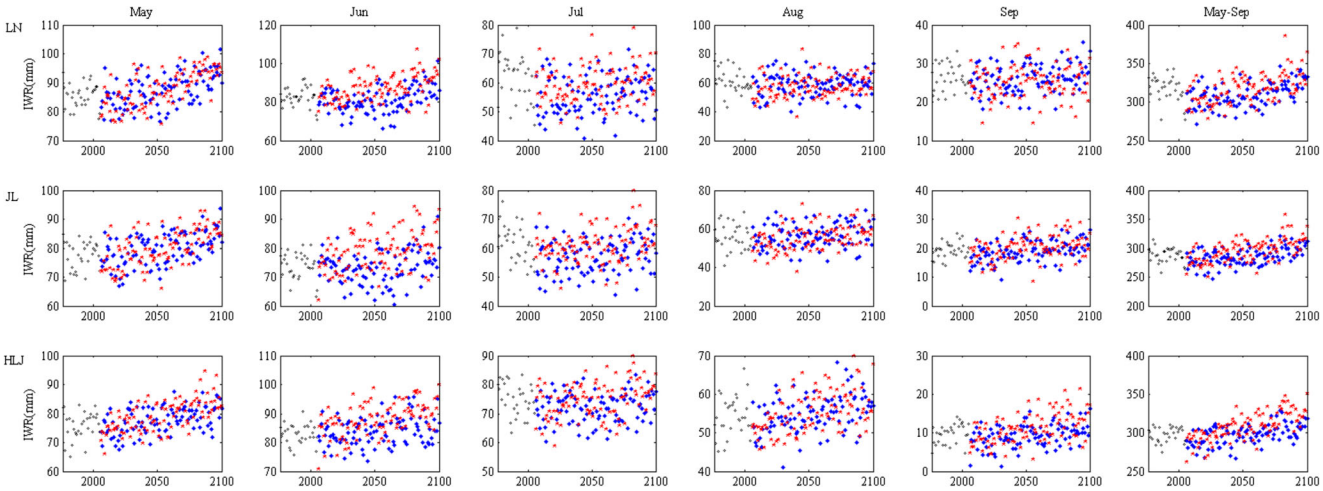

Fig. 5 Yearly variation of IWR in provinces (black, blue, and red scatters represent baseline, RCP4.5, and RCP8.5, respectively)

been confirmed by studies that employed the simple water balance model using the CMIP5 datasets as inputs (Wada et al. 2013). Due to increasing temperatures, elevated CWR values were identified for different types of rice across different cultivated regions under future scenarios (Wang et al. 2014, 2017; Ding et al. 2017). Under future climate scenarios relative to the past decades, temperature increases during the growing season for rice resulted in higher CWR (Cong et al. 2011). By using crop models to simulate future rice growth, an increasing IWR was also detected that was due to higher CWR caused by increased temperature (Boonwichai et al. 2018). Relative to baseline, the percent change of CWR in 2070–2099 was larger than that in 2021–2040, and the difference was larger than that change of EP. In addition, CWR and EP changes were greater under RCP8.5 than RCP4.5, and were attributed to IWR changes, consistent with previous reports (Boonwichai et al. 2018). The latter highlighted more severe temperature rises thereby increasing evaporation as well as CWR although EP was still expected to increase in the future.

The consequences of IWR-related results presented above were derived using a single rice variety (Wang et al. 2017). This was applied with the use of a developing growing phenology to calculate phenological period and further assess the impacts of climate change on IWR for rice (Ding et al. 2017). However, the growing period for rice would most likely change with altered climate conditions and the average growth duration for rice would be shortened under warming conditions. For example, the rice growing season in 2010–2050 would be reduced by 4.7 and 5.8 days under the SRES A2 and B2 scenarios, respectively (Zhang et al. 2015). Thus, strategies such as taking mid-late-maturing rice cultivars to replace early-maturing ones and breeding new rice cultivars with higher thermal requirements have been proposed to lessen the impact on yields (Wu et al. 2014; Zhang et al. 2017). Our findings for the use of a stabilized time period of May–Sep for rice growth might be an alternative way as thermal requirements for rice varieties would vary with climate alterations.

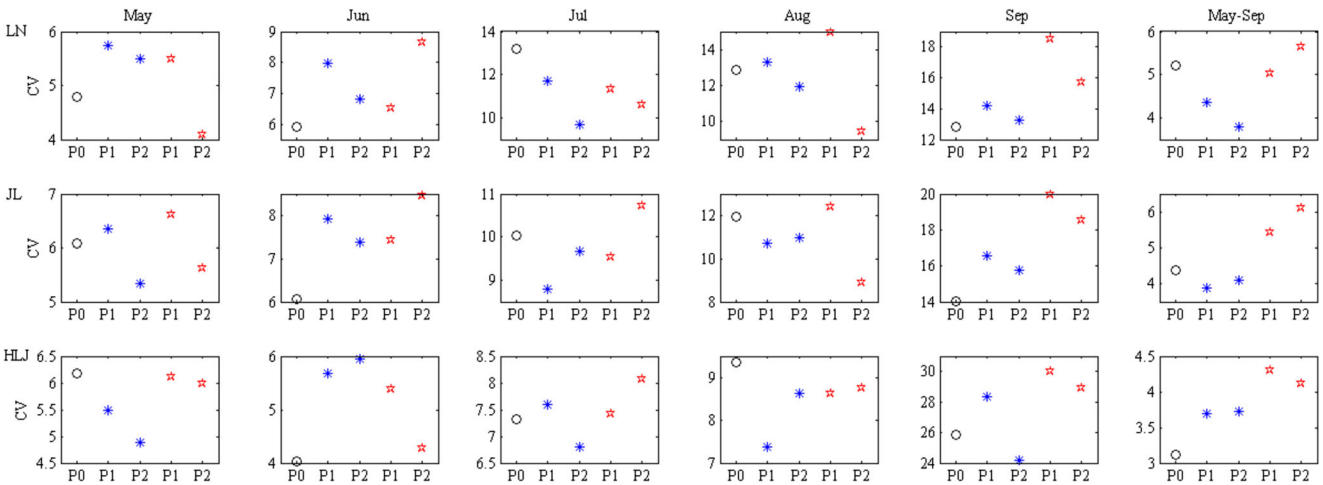

Fig. 6 Coefficient of variance for IWR in provinces (black, blue, and red scatters represent baseline, RCP4.5, and RCP8.5, respectively; P0, P1, and P2 represent 1976–2005, 2036–2065, and 2070–2099, respectively)

Table 2 EP in baseline and percent change in future periods relative to baseline in provinces

Province	Period	P0 (mm)	RCP4.5 (%)		RCP8.5 (%)	
			P1 (%)	P2	P1	P2
LN	May	32.58	16.70	10.53	23.32	24.74
	Jun	51.34	18.18	13.80	9.54	18.71
	Jul	76.64	14.73	15.49	13.28	21.81
	Aug	64.68	14.80	15.82	17.73	25.25
	Sep	32.80	13.63	14.14	16.74	29.71
	May–Sep	258.04	15.54	14.44	15.36	23.43
JL	May	35.94	13.30	11.39	21.24	25.16
	Jun	57.90	15.23	13.47	8.02	17.00
	Jul	76.75	12.78	13.55	11.61	17.74
	Aug	63.31	10.93	11.09	13.47	20.79
	Sep	33.47	11.23	12.22	10.94	19.55
	May–Sep	267.36	12.75	12.49	12.48	19.53
HLJ	May	32.85	14.06	14.85	18.68	26.38
	Jun	52.51	11.73	13.59	9.76	17.80
	Jul	67.65	13.80	14.58	12.64	19.70
	Aug	61.27	10.05	10.44	11.39	20.54
	Sep	37.20	10.89	11.14	10.70	13.99
	May–Sep	251.48	12.06	12.89	12.23	19.53

Table 3 CWR in baseline and percent change in future periods relative to baseline in provinces

Province	Period	P0 (mm)	RCP4.5 (%)		RCP8.5 (%)	
			P1 (%)	P2	P1	P2
LN	May	118.32	4.95	7.50	6.52	12.82
	Jun	134.08	3.88	7.72	6.95	12.55
	Jul	138.29	3.26	6.20	5.89	11.17
	Aug	125.57	4.71	7.03	6.48	11.38
	Sep	59.12	6.65	8.93	9.12	14.47
	May–Sep	575.38	4.42	7.28	6.73	12.21
JL	May	113.56	5.58	8.22	7.13	13.71
	Jun	131.89	4.21	7.69	7.29	12.92
	Jul	138.24	3.40	5.90	5.76	10.85
	Aug	119.22	5.01	7.75	6.88	12.55
	Sep	52.70	7.33	10.02	10.28	16.82
	May–Sep	555.63	4.76	7.59	7.07	12.86
HLJ	May	108.89	5.67	8.10	7.30	14.32
	Jun	135.48	4.64	7.24	7.43	12.96
	Jul	142.72	3.56	5.64	5.79	10.78
	Aug	115.66	5.26	8.10	7.58	13.32
	Sep	47.01	7.62	10.51	10.81	18.59
	May–Sep	549.75	4.95	7.46	7.30	13.22

IWR projections under climate change were plagued by some inevitable uncertainties. Firstly, although downscaling and ensemble methods reduce bias relative to individual GCMs, inherited uncertainties that originated from emission scenarios and parameterization schemes would not be totally removed (Ning et al. 2012). In addition, more precise GCM simulations lead to decreased uncertainty and more reliable potential IWR predictions. Methods accessing IWR were primarily based on simple assumptions and ignored some uncertainties such as assuming that the rice crop coefficient would be stable same to an inherent assumption in crop simulation models. However, this would not be appropriate here since rice varieties would be altered with changing climate conditions. Up to now there was no satisfactory way to solve this problem and thus the assumption was generally accepted.

5 Conclusion

Exploring the potential impact of climate change on IWR is of great importance for the sustainability of water and rice production. Fine-resolution temperature and precipitation datasets from 20 downscaled GCMs were successfully applied in the Hargreaves model to estimate ET and to systematically assess the potential IWR dynamic for rice across NEC. IWR predictions decreased from southwestern HLJ and western JL to the southeastern and northeastern areas for total growing times in baseline and future periods. In particular, IWR ranked by months was Jun > May > Jul > Aug > Sep. IWR displayed an increasing trend from east to west across the study region and was larger under RCP8.5 relative to RCP4.5. The provincial IWR indicated a positive change in 2070–2099 under RCP4.5 as well as in 2036–2065 and 2070–2099 under RCP8.5. The IWR changes were ranked as HLJ > JL > LN. The change of IWR in May–Sep in 2070–2099 under RCP8.5 relative to baseline was more than 2 times greater than that under RCP4.5. These current and potential changes of IWR suggested that special adaptive strategies should be implemented in different areas across NEC.

Funding This study was co-funded by the National Key Research and Development Plan of China [2018YFC1507802, 2017YFD03001, 2017YFC1502402].

References

Boonwichai S, Shrestha S, Babel M, Weesakul S (2018) Climate change impacts on irrigation water requirement, crop water productivity and rice yield in the Songkhram River Basin, Thailand. J Clean Prod 198:1157–1164. https://doi.org/10.1016/j.jclepro.2018.07.146

Bormann H (2011) Sensitivity analysis of 18 different potential evapotranspiration models to observed climatic change at German climate stations. Clim Chang 104:729–753. https://doi.org/10.1007/s10584-010-9869-7

Boudhina N, Masmoudi MM, Alaya I, Jacob J, Mechlia NB (2019) Use of AquaCrop model for estimating crop evapotranspiration and biomass production in hilly topography. Arab J Geosci 12:259. https://doi.org/10.1007/s12517-019-4434-9

Cong Z, Yao B, Ni G (2011) Cropwater demand in China under the SRA1B emissions scenario. Adv Water Sci 22:38–43 CNKI:32-1309/P.20110115.2245.013

Ding YM, Wang WG, Song RM, Shao QX, Jiao XY, Xing WQ (2017) Modeling spatial and temporal variability of the impact of climate change on rice irrigation water requirements in the middle and lower reaches of the Yangtze River, China. Agric Water Manag 193:89–101. https://doi.org/10.1016/j.agwat.2017.08.008

Ding YM, Wang WG, Zhuang QL, Luo YF (2020) Adaptation of paddy rice in China to climate change: the effects of shifting sowing date on yield and irrigation water requirement. Agric Water Manag 228: 105890. https://doi.org/10.1016/j.agwat.2019.105890

Döll P, Siebert S (2002) Global modeling of irrigation water requirements. Water Resour Res 38:8-1–8-10. https://doi.org/10.1029/2001wr000355

Donat MG, Lowry AL, Alexander LV, O'Gorman P, Mahe N (2017) More extreme precipitation in the world's dry and wet regions. Nat Clim Chang 7:154–158. https://doi.org/10.1038/NCLIMATE2941

Donohue RJ, McVicar TR, Roderick ML (2010) Assessing the ability of potential evaporation formulations to capture the dynamics in evaporative demand within a changing climate. J Hydrol 386:186–197. https://doi.org/10.1016/j.jhydrol.2010.03.020

Fan W, Xiao CL, Xiong QH, Liang XJ (2009) Study on sustainability assessment of groundwater function in plain area of Jilin province. Water Resour Protect 25:14–17 http://www.docin.com/p-1197270202.html. Accessed 15 Jan 2020

FAO (2020) Food and Agricultural Organization of the United Nations. FAOSTAT: available at: http://www.fao.org/faostat/en/#data/QC. Accessed 10 Aug 2020

Feng Y, Jia Y, Cui NB, Zhao L, Chen L, Gong DZ (2017) Calibration of Hargreaves model for reference evapotranspiration estimation in Sichuan basin of southwest China. Agric Water Manag 181:1–9. https://doi.org/10.1016/j.agwat.2016.11.010

Gao X, Schlosser A, Fant C, Strzepek K (2018) The impact of climate change policy on the risk of water stress in southern and eastern Asia. Environ Res Lett 13:064039. https://doi.org/10.1088/1748-9326/aaca9e

Gosling S, Arnell N (2016) A global assessment of the impact of climate change on water scarcity. Clim Chang 134:371–385. https://doi.org/10.1007/s10584-013-0853-x

Han HH, Cui YL, Huang Y, Wang SP, Duan QC, Zhang L (2019) Impacts of the channel/barrier effect and three-dimensional climate-a case study of rice water requirement and irrigation quota in Yunnan, China. Agric Water Manag 212:317–327. https://doi.org/10.1016/j.agwat.2018.09.017

Hargreaves GH, Allen RG (2003) History and evaluation of Hargreaves evapotranspiration equation. J Irrig Drain Eng 129:53–63. https://doi.org/10.1061/(ASCE)0733-9437(2003)129:1(53)

He HB, Ma FY, Yang R, Chen L, Jia B, Cui J, Fan H, Wang X, Li L (2013) Rice performance and water use efficiency under plastic mulching with drip irrigation. PLoS One 8:e83103. https://doi.org/10.1371/journal.pone.0083103

Huang ZG, Wang XL, Xiao Y, Yang F, Wang CX (2015) Effect of climate change on rice irrigation water requirement in Songnen Plain, Northeast China. Chin J Appl Ecol 26:260–268 http://www.cjae.net/CN/Y2015/V26/I1/260. Accessed 5 Feb 2020

Li T, Hasegawa T, Yin XY, Zhu Y, Boote K, Adam M, Bregadlio S, Buis S (2015) Uncertainties in predicting rice yield by current crop models under a wide range of climatic conditions. Glob Chang Biol 21:1328–1341. https://doi.org/10.1111/gcb.12758

Liu WB, Sun FB (2016) Assessing estimates of evaporative demand in climate models using observed pan evaporation over China. J Geophys Res Atmos 121:8329–8349. https://doi.org/10.1002/2016JD025166

Mancosu N, Spano D, Orang M, Sarreshteh S, Snyder RL (2016) SIMETAW# - a model for agricultural water demand planning. Water Resour Manag 30:541–557. https://doi.org/10.1007/s11269-015-1176-7

Nie ZT, Zhang ZX, Qi ZJ, Chen P, Lin YN, Sun ZY (2019) Spatial and temporal distribution characteristics of rice water requirement in Heilongjiang province during 1960-2015. Trans CSAM 50:279–290. https://doi.org/10.6041/j.issn.100-12989.2019.05.032

Ning L, Mann ME, Crane R, Wagener T, Najjar RG, Singh R (2012) Probabilistic projections of anthropogenic climate change impacts on precipitation for the mid-Atlantic region of the United States. J Clim 25:5273–5291. https://doi.org/10.1175/jcli-d-11-00565.1

Sangelanton L, Russo A, Gennaretti F (2019) Impact of bias correction and downscaling through quantile mapping on simulated climate change signal: a case study over Central Italy. Theor Appl Climatol 135:725–740. https://doi.org/10.1007/s00704-018-2406-8

Schaldach R, Koch J, Beek TAD, Kynast E, Flörke M (2012) Current and future irrigation water requirements in pan-Europe: an integrated analysis of socio-economic and climate scenarios. Glob Planet Chang 94-95:33–45. https://doi.org/10.1016/j.gloplacha.2012.06.004

Sen P (1968) Estimates of the regression coefficient based on Kendall' s tau. J Am Stat Assoc 63:1379–1389. https://doi.org/10.1080/01621459.1968.10480934

Shahid S (2011) Impact of climate change on irrigation water demand of dry season Boro rice in northwest Bangladesh. Clim Chang 105: 433–453. https://doi.org/10.1007/s10584-010-9895-5

Thiel H (1950) A rank-invariant method of linear and polynomial regression analysis, part 3. Proceedings of Koninalijke Nederlandse Akademie van Weinenschatpen, Series A Mathematical Sciences 53:1397–1412. https://doi.org/10.1007/978-94-011-2546-8_20

Thrasher B, Maurer E, McKellar C, Duffy PB (2012) Technical note: Bias correcting climate model simulated daily temperature extremes with quantile mapping. Hydrol Earth Syst Sci 16:3309–3314. https://doi.org/10.5194/hess-16-3309-2012

Wada YD, Wisser S, Florke M, Gerten D, Haddeland I, Hanasaki N, Masaki Y, Portmann FT, Stacke T, Tessler Z, Schewe J (2013) Multimodel projections and uncertainties of irrigation water demand under climate change. Geophys Res Lett 40:4626–4632. https://doi.org/10.1002/grl.50686

Wang WG, Yu Z, Zhang W, Shao W, Zhang Q, Luo YF, Jiao Y, Xu X (2014) Responses of rice yield, irrigation water requirement and water use efficiency to climate change in China: historical simulation and future projections. Agric Water Manag 146:249–261. https://doi.org/10.1016/j.agwat.2014.08.019

Wang XH, Xu YJ, Zhang GX, Qu W, Cheng WG (2016) The positive impacts of irrigation schedules on rice yield and water consumption: synergies in Jilin province, Northeast China. Inter J Agric Sus 14:1–12. https://doi.org/10.1080/14735903.2015.1010305

Wang WG, Ding YM, Shao QX, Xu JZ, Jiao XY, Luo YF, Yu ZB, Tao E (2017) Bayesian multi-model projection of irrigation requirement and water use efficiency in three typical rice plantation region of China based on CMIP5. Agric For Meteorol 232:89–105. https://doi.org/10.1016/j.agrformet.2016.08.008

Werner AT, Cannon AJ (2015) Hydrologic extremes-an intercomparison of multiple gridded statistical downscaling methods. Hydrol Earth Syst Sci 12:6179–6239. https://doi.org/10.5194/hess-20-1483-2016

Wu W, Fang Q, Ge Q, Zhou M, Lin Y (2014) CERES-Rice model-based simulations of climate change impacts on rice yields and efficacy of adaptive options in Northeast China. Crop Pasture Sci 35:1267–1277. https://doi.org/10.1071/CP14009

Ye Q, Yang XG, Dai SW, Chen GS, Li Y, Zhang CC (2015) Effects of climate change on suitable rice cropping areas, cropping systems and crop water requirements in southern China. Agric Water Manag 159:35–44. https://doi.org/10.1016/j.agwat.2015.05.022

Yu GM, Yang YM, Tu ZF, Jie Y, Yu QW, Hu XY, Yu HL, Zhou RR, Chen XX, Wang HZ (2016) Modeling the water-satisfied degree for production of the main food crops in China. Sci Total Environ 547:215–225. https://doi.org/10.1016/j.scitotenv.2015.12.105

Zhang QT, Xia Q, Liu CCK, Geng S (2013) Technologies for efficient use of irrigation water and energy in China. J Integr Agric 12:1363–1370. https://doi.org/10.1016/S2095-3119(13)60544-4

Zhang J, Feng L, Zou H, Liu D (2015) Using ORYZA2000 to model cold rice yield response to climate change in the Heilongjiang province, China. Crop J 3:317–327. https://doi.org/10.1016/j.cj.2014.09.005

Zhang Q, Zhang W, Li TT, Sun WJ, Yu YQ, Wang GC (2017) Projective analysis of staple food crop productivity in adaptation to future climate change in China. Int J Biometeorol 61:1445–1460. https://doi.org/10.1007/s00484-017-1322-4

Zhang L, Xu YL, Meng CC, Li XH, Wang CG (2020a) Comparison of statistical and dynamic downscaling techniques in generating high-resolution temperature in China from CMIP5 GCMs. J Appl Meteorol Climatol 59:207–235. https://doi.org/10.1175/JAMC-D-19-0048.1

Zhang L, Yang BY, Li S, Guo AH, Huo ZG (2020b) Potential dry/wet dynamic in China under RCP scenarios. Theor Appl Climatol 141:443–454. https://doi.org/10.1007/s00704-020-03193-5

Zhao T, Dai A (2017) Uncertainties in historical changes and future projections of drought. Part II: model-simulated historical and future drought changes. Clim Chang 144:535–548. https://doi.org/10.1007/s10584-016-1742-x

Zhu XF, Zhao AZ, Li YZ, Liu XF (2015) Agricultural irrigation requirements under future climate scenarios in China. J Arid Land 7:224–237. https://doi.org/10.1007/s40333-014-0080-y